Supporting Information

Dual photoresponsive & water-triggered nitric oxide releasing materials based on rhodium-based metal-organic polyhedra

Francisco J. Carmona,[a,†] Thiago Negrao Chuba, [a,c] Eli Sanchez-Gonzalez,[a] Jenny Pirillo, [d] Yuh Hijikata, [e] Shuhei Furukawa*[a,b]

[a]Institute for Integrated Cell-Material Sciences (WPI-iCeMS), Kyoto University, Yoshida, Sakyo-ku, Kyoto 606-8501, Japan

[b]Department of Synthetic Chemistry and Biological Chemistry, Graduate School of Engineering, Kyoto University, Katsura, Nishikyo-ku, Kyoto 615-8510, Japan

[c]Graduate School of Advanced Integrated Studies in Human Survivability, Kyoto University, Yoshida, Sakyo-ku, Kyoto 606-8306, Japan.

[d]Department of Chemistry and Biotechnology, School of Engineering, and Department of Materials Chemistry, Graduate School of Engineering, Nagoya University, Chikusa-ku, Nagoya 464-8603, Japan

[e]Research Center for Net Zero Carbon Society, Institute of Innovation for Future Society, Nagoya university, Chikusa-ku, Nagoya, 464-8601, Japan

EXPERIMENTAL SECTION

Instrumentation. All reagents were purchased from Wako Pure Chemical Industries and were used without further purification. PXRD measurements were performed using a Rigaku Smartlab (Dtex Ultra detector) operating with a rotating anode Cu Kα X-ray generator (λ = 1.54 Å) with a 40 kV beam voltage and 200 mA current. The supercritical CO_2 drying process was carried out on SCLEAD-2BD autoclave (KISCO) using supercritical CO_2 at 14 MPa and 313 K. The CO_2 sorption isotherms were recorded on a BELSORP-mini volumetric adsorption instrument from BEL Japan, Inc at 195 K. The nitric oxide isotherms were collected on a BELSORP-max volumetric adsorption instrument from BEL Japan, Inc. at 298 K. In all cases, the materials were activated (393 K, 10^{-2} Pa) during 12 hours prior to the measurement. Infrared (IR) spectroscopy data were recorded using a Jasco FT/IR-6100 with a 1 cm^{-1} resolution and an accumulation of 64 scans. The samples were observed using a field-emission scanning electron microscope with a JEOL Model JSM-7001F4 system operating at 5 kV and 5 mA current. ^{1}H-NMR spectra were recorded on a Bruker Biospin DRX-600 (600 MHz) spectrometer. Dynamic Light Scattering measurements were performed using a Malvern Zetasizer Nano ZS. The UV-Vis absorption and diffuse reflectance spectra were collected using a Jasco (V-750) spectrophotometer with an integrating sphere (ISV-922). For the diffuse reflectance spectra, 4 mg of the sample were grinded with 150-200 mg of CaF_2 until getting a homogenous mixture. The powder was transferred to the sample holder and the spectra were collected.

Synthesis of 1,4-bis(imidazol-1-ylmethyl)benzene (bix). The preparation was carried out as previously reported.[1] Imidazole (2.13g, 16.6 mmol) and NaH (0.88 g of 60% in mineral oil) were mixed in 50 mL of tetrahydrofuran (THF) for 30 min. Then, a solution of 1,4-bis(bromomethyl)benzene (2 g, 7.57 mmol) in 20 ml of THF was added and the mixture was heated

at 323 K during 4 h. The reaction was quenched by adding ice water (25 ml) and the organic phase extracted with chloroform, treated with anhydrous $MgSO_4$ and dried under vacuum. The white powder was washed with diethyl ether twice and dried under vacuum. The purity of the compound was certified by NMR spectroscopy (Figure S1).

Synthesis of C$_{12}$RhMOP. The synthesis of **C$_{12}$RhMOP** was adapted from a previously reported protocol.[2] In a typical synthesis, rhodium acetate $Rh_2(AcO)_4 \cdot (MeOH)_2$ (0.2 g, 0.40 mmol) and 5-dodecoxybenzene-1,3-dicarboxylic acid (H_2BDC-C_{12}) (0.348 g, 0.99 mmol) were dissolved in 20 ml of N,N-dimethylacetamide (DMA). Then, Na_2CO_3 (0.104 g, 0.99 mmol) was added and the suspension was heated at 373 K for 24 h in a pre-heated oven. The resulting green solution was filtered to remove the carbonate. The liquid phase was treated with MeOH to precipitate C_{12}RhMOP and the solid was recovered by centrifugation. The material was suspended in EtOH (12 h) and MeOH (12 h) to exchange the DMA from the pore. Afterwards, the solid was re-dissolved in dichloromethane, filtered and evaporated under low-pressure. Finally, the solid was recovered by centrifugation and dried overnight at 393 K under vacuum. The purity of the compound was certified by NMR spectroscopy (Figure S2).

Synthesis of C$_{12}$RhMOP-biz. The synthesis of **C$_{12}$RhMOP-biz** was adapted from a previously reported protocol.[2] A solution of **C$_{12}$RhMOP** (50 mg, 4.6 10^{-3} mmol) in 10 mL of N,N-dimethylformamide (DMF) was mixed with a solution of 1-benzylimidazole (biz) (10 mg, 0.06 mmol) in 1 mL of DMF (biz excess of 13 eq.mol) and stirred during 10 min at room temperature. The purple solution was treated with MeOH to precipitate **C$_{12}$RhMOP-biz**. The solid was collected by centrifugation after being washed twice with MeOH. Finally, the material was dried under air.

Synthesis of coordination polymer particles (C$_{12}$RhMOP-CPP). A solution of **C$_{12}$RhMOP** (20 mg, 1.8 10^{-3} mmol) in 1.21 mL of DMF was titrated at 308 K with a solution of bix in DMF (12.5 mol eq. mL^{-1}). Specifically, 0.5 mol eq. (40 µL) of bix solution were added every 5 min until reaching 6 mol eq. The purple suspension was washed twice in DMF and acetone and the solid was collected by centrifugation. The resulting particles were dried with supercritical CO$_2$ at 14 MPa and 313 K for 90 min.

Loading of the materials with NO: C$_{12}$RhMOP, C$_{12}$RhMOP-biz and **C$_{12}$RhMOP-CPP** were loaded with NO by using a BELSORP-max volumetric adsorption instrument from BEL Japan, Inc. In a typical experiment, c.a. 100 mg of each material were firstly activated at 393 K and 10^{-2} Pa. Afterwards, the materials were loaded with NO at 298 K and P$_{NO}$ = 101.3 kPa until the equilibrium was reached. Finally, the samples were evacuated under vacuum (10^{-2} Pa) to remove the potential NO molecules physisorbed inside the pores. The materials were stored under an inert atmosphere to avoid an unwanted release of NO.

Sample digestion for NMR measurement. 10 mg of both **C$_{12}$RhMOP-biz** and **C$_{12}$RhMOP-CPP** were dispersed in 750 µL of DMSO-d6 and 20 µL of DCl. The suspension was heated at 373 K during 12 hours, resulting in a yellow solution.

Computational studies. Similarly to the previous work[3], we employed Rh$_2$(HCO$_2$)$_4$ for the model of Rh open metal site, Rh$_2$(HCO$_2$)$_4$(NO)$_2$ and Rh$_2$(HCO$_2$)$_4$(NO) for the NO adsorbed model. In addition, Rh$_2$(HCO$_2$)$_4$(NO)(Me-Im) and Rh$_2$(HCO$_2$)$_4$(Me-Im) (Me-Im = 1-methyleimidazole) were also employed to evaluate the binding energy of NO (Figure S8). All calculations were conducted using the density functional theory (DFT) method with the M06L functional[4]. The Stuttgart-Dresden-Bonn basis set was used for Rh, where the core electrons were replaced with the

effective core potential of Stuttgart-Dresden-Bonn[5]. The 6-311G(2d) basis sets were used for both of NO and Me-Im. The 6-311G(d) basis sets were used for the other atoms with the diffuse function for the O of formate. Geometry optimization without any symmetries and frequency calculations were performed with the Gaussian 16 program Package[6].

Because Rh dimer of a paddle wheel takes singlet state in the ground state, we calculated $Rh_2(HCO_2)_4$ in the singlet state. On the other hand, a π^* orbital of NO has one unpaired electron, which can form an electron pair with an electron in Rh orbital, and the doublet state for $Rh_2(HCO_2)_4(NO)$ and $Rh_2(HCO_2)_4(NO)(Me\text{-}Im)$ and the singlet state for $Rh_2(HCO_2)_4(NO)_2$ and $Rh_2(HCO_2)_4(Me\text{-}Im)$ were employed as the ground states in this work. The binding energies (E_b) of the gases are defined as follows;

$$E_b = -\{E[Rh_2(HCO_2)_4(X)(NO)] - (E[Rh_2(HCO_2)_4(X)] + E[NO])\},$$

where X = MeIm or NO, and E are energies at the optimized structures of each molecule. Basis set superposition error (BSSE) was corrected using the counterpoise method[7].

Assessment of chemical stability under anhydrous and dark conditions. Solutions of both **C$_{12}$RhMOP+NO** and **C$_{12}$RhMOP-biz+NO** (0.07 mM, 2 mL) in degassed dry toluene were freshly prepared in a sealed quartz cuvette under an inert atmosphere and were kept in the dark. At different times, the UV-Vis spectra of the solutions were collected to assess if nitric oxide is released from the MOPs.

Assessment of chemical stability under light irradiation. Solutions of both NO-loaded **C$_{12}$RhMOP** and **C$_{12}$RhMOP-biz** (0.07 mM, 2 mL) in degassed toluene was freshly prepared in a sealed quartz cuvette under inert atmosphere. The sample was irradiated with a 300-W Xenon

lamp (Asahi Spectra Max-303 equipped with a 300- to 600-nm ultraviolet–visible module and x 1.0 collimator lens, distance cuvette-lamp of 15 cm). At different times, the solution was analysed by means of UV−vis spectroscopy to assess the nitric oxide release induced by light.

Photoresponsive release of nitric oxide in solid state. Suspensions of the materials $C_{12}RhMOP+NO$, $C_{12}RhMOP-biz+NO$ and $C_{12}RhMOP-CPP+NO$ in hexane (*c.a.* 1 mg mL^{-1}) were repeatedly spin-coat (150 rpm) in an 18 x 18 cover slip and activated under reduced pressure for 30 min (10 mbar, 298 K). The weight of the coated material was determined by using a precision scale (typically 60-100 μg). The samples were placed in a custom-made cell and irradiated 300-W Xenon lamp (Asahi Spectra Max-303 equipped with a 300- to 600-nm ultraviolet–visible module and x 1.0 collimator lens, distance cuvette-lamp of 15 cm, 50 % of irradiation power). The NO release measurements were performed using a Sievers NOA 280i chemiluminescence NO analyser. The instrument was calibrated by passing nitrogen with a content of NO < 1 ppb and 600 ppb of NO gas. Nitrogen was used as a carrier with a flow rate of 200 mL min^{-1}.

Water-triggered release of nitric oxide in solid state. The sample preparation was carried out similarity to the analysis of NO-release under photoactivation. However, the nitrogen flow was saturated with water before entering in the sample-chamber by passing through a water column. Likewise, the sample chamber was protected from the light to avoid an unwanted photoresponsive release of NO.
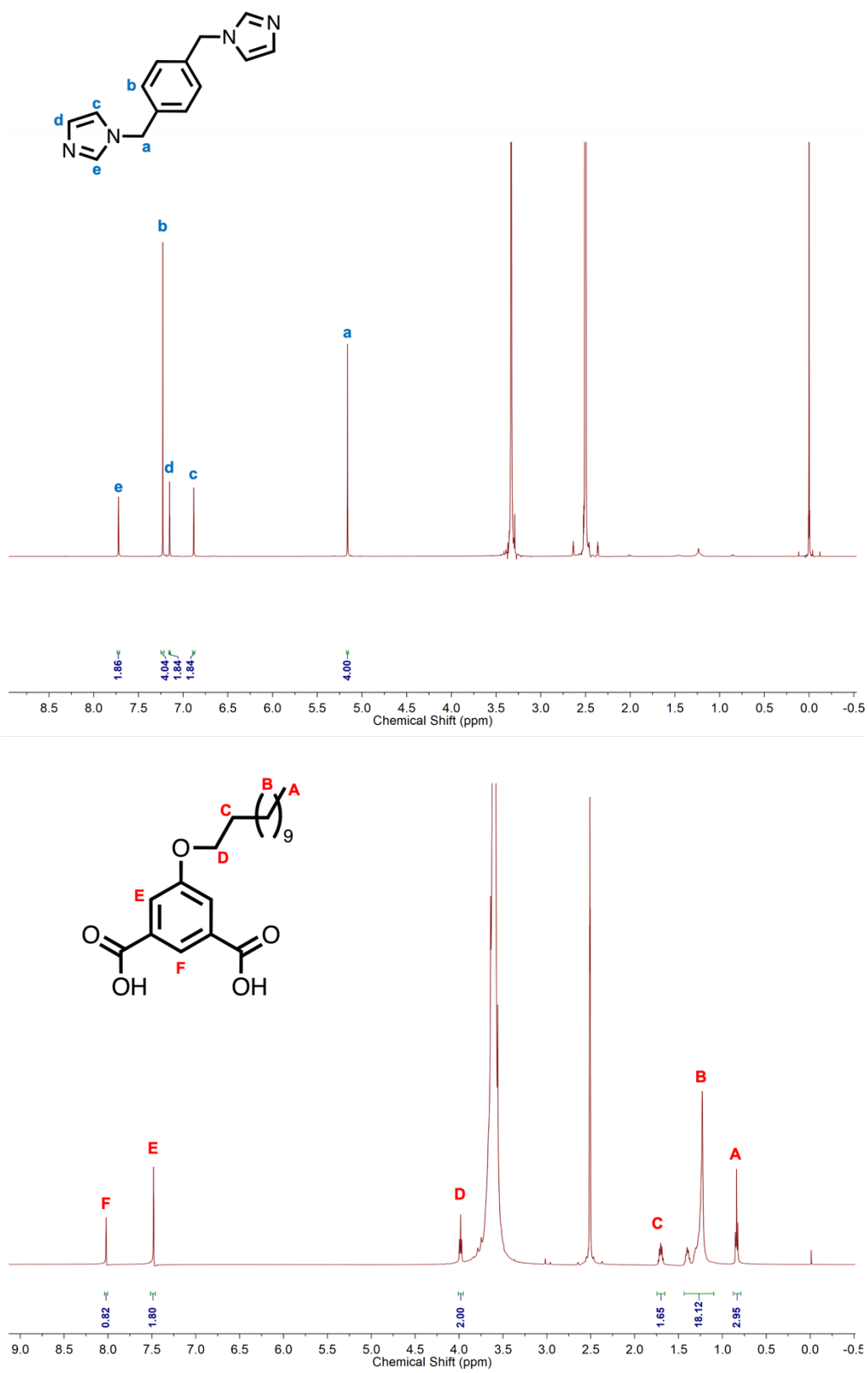
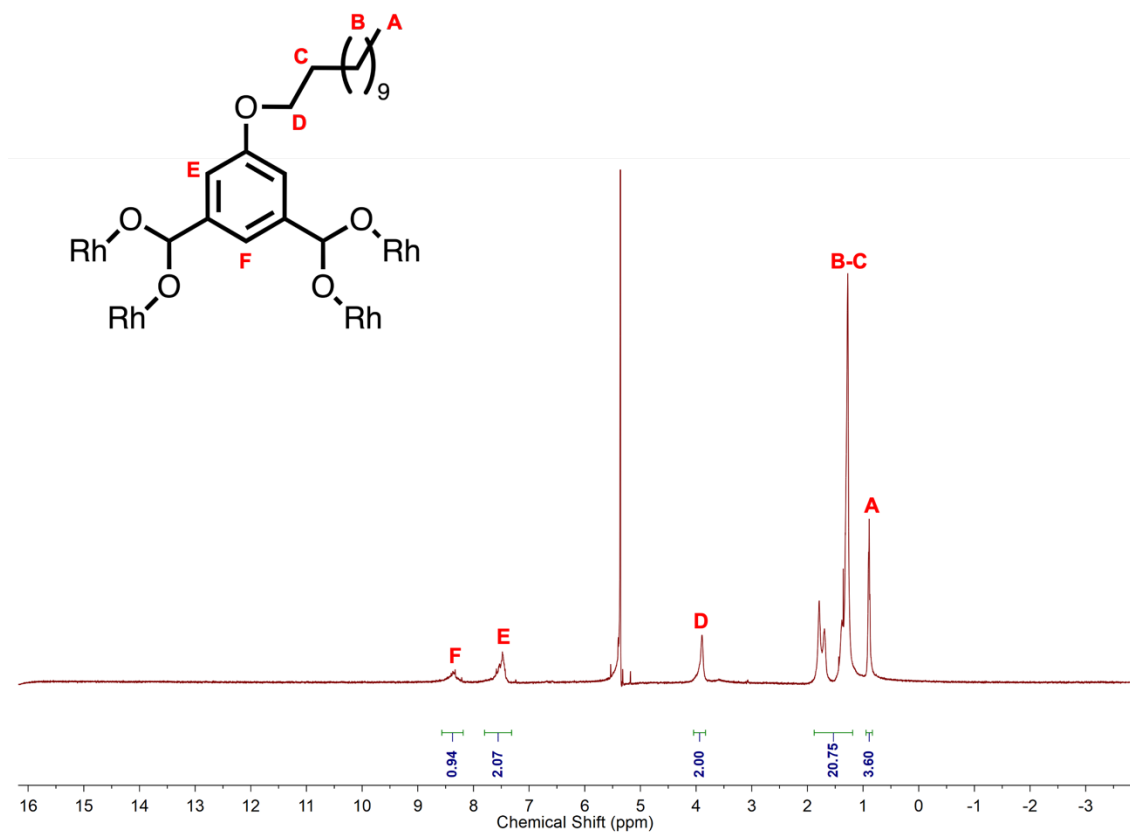**Figure S1.** ^{1}H-NMR spectrum of: a) bix in DMSO-d6 and b) H_2BDC-C_{12} in DMSO-d6.

Figure S2. ^{1}H-NMR spectrum of **C$_{12}$RhMOP** in CD$_2$Cl$_2$.
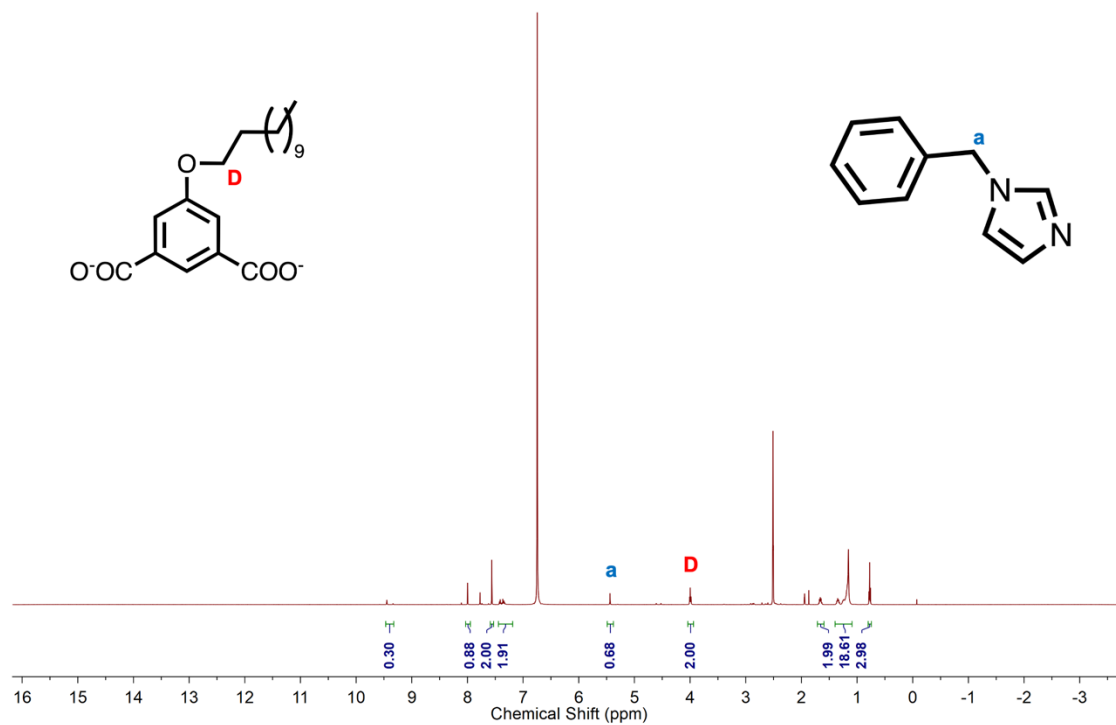
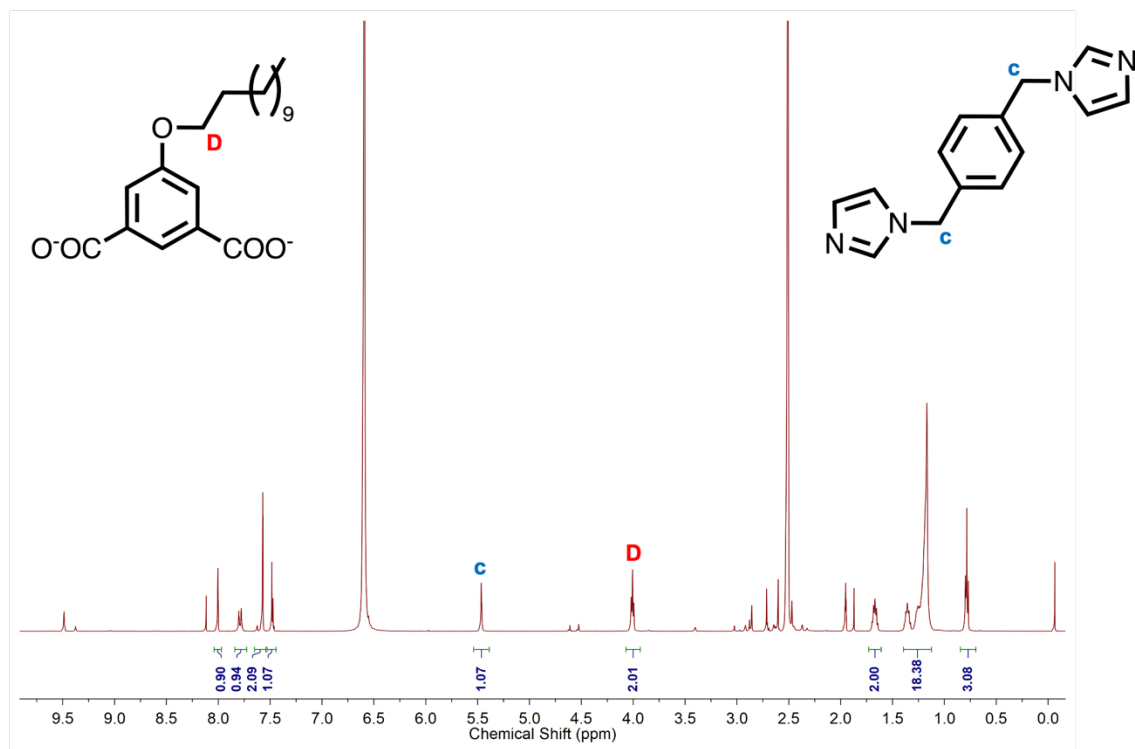**Figure S3.** ^{1}H-NMR spectrum of **C$_{12}$RhMOP-biz** digested with DMSO-d6 and DCl.

Figure S4. ^{1}H-NMR spectrum of **C$_{12}$RhMOP-CPP** digested with DMSO-d6 and DCl.

Table S1. Loading of NO determined and open metal sites available for $C_{12}RhMOP$, $C_{12}RhMOP$-biz and $C_{12}RhMOP$-CPP.

Sample	Formula of framework	mmol NO per Rh$_2$ paddle wheel[a]	OMSs per Rh$_2$ paddle wheel[b]
$C_{12}RhMOP$+NO	$[Rh_2(C_{12}bdc)_2]_{12}$	2.0	2.0
$C_{12}RhMOP$-biz+NO	$[Rh_2(C_{12}bdc)_2]_{12}(biz)_{8.1}$	1.3	1.3
$C_{12}RhMOP$-CPP+NO	$[Rh_2(C_{12}bdc)_2]_{12}(bix)_{0.5}]_{12}$	1.0	1.0

[a]Determined by NO-adsorption isotherm. [b]Determined by NMR.

Table S2. NO-payload of the material prepared in comparison with other porous materials with open metal sites proposed as NO-releasing frameworks.

| Sample	Formula of framework	Payload (mmol g^{-1})	Reference
$C_{12}RhMOP$+NO	$[Rh_2(C_{12}bdc)_2]_{12}$	2.1	This work
$C_{12}RhMOP$-biz+NO	$[Rh_2(C_{12}bdc)_2]_{12}(biz)_{8.1}$	1.3	This work
$C_{12}RhMOP$-CPP+NO	$[Rh_2(C_{12}bdc)_2]_{12}(bix)_{0.5}]_{12}$	1.0	This work
HKUST-1	$Cu_3(btc)_2$	2.2	[8]
Co-CPO	$Co_2(dhtp)$	6.0	[9]
Ni-CPO	$Ni_2(dhtp)$	7.0	
MIL-88-A	$FeOX(fumarate)_3$	2.5	[10]
MIL-88-B	$Fe_3OX(bdc)_3$	1.6	
MIL-88-B-NO2	$Fe_3OX(NO_2bdc)_3$	1.0	
MIL-88-B-2OH	$Fe_3OX(dhtp)_3$	1.0	
$Fe_2(dobdc)$	$Fe_2(dhtp)$	6.2	[11]
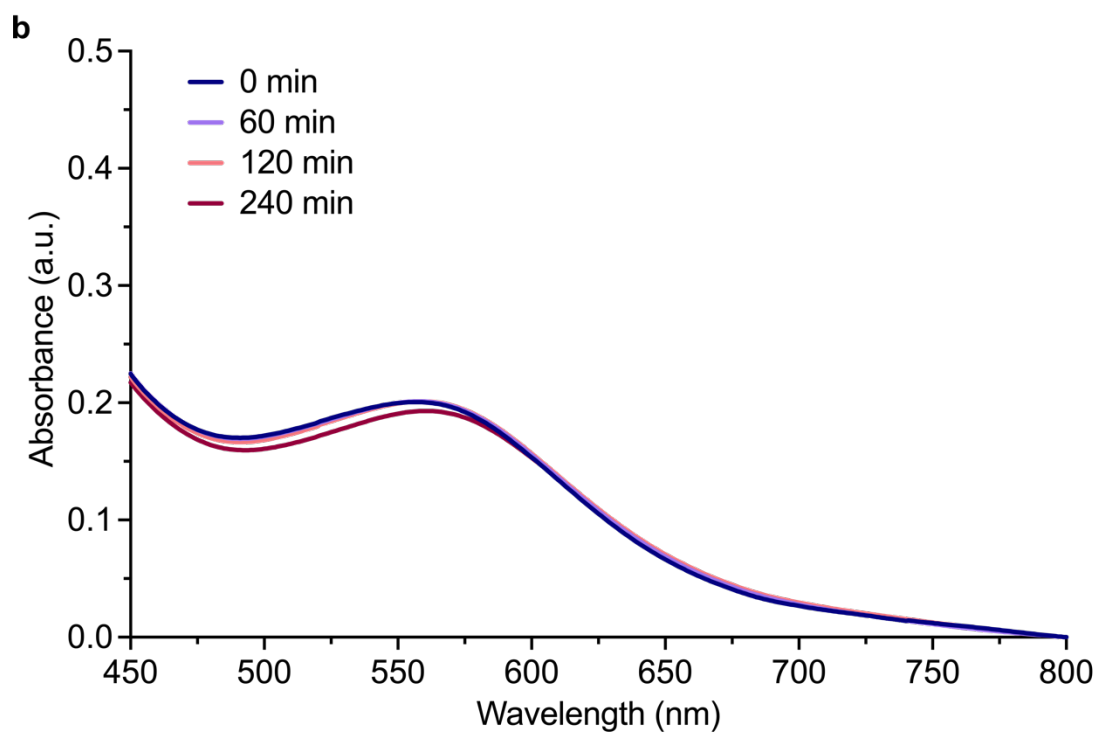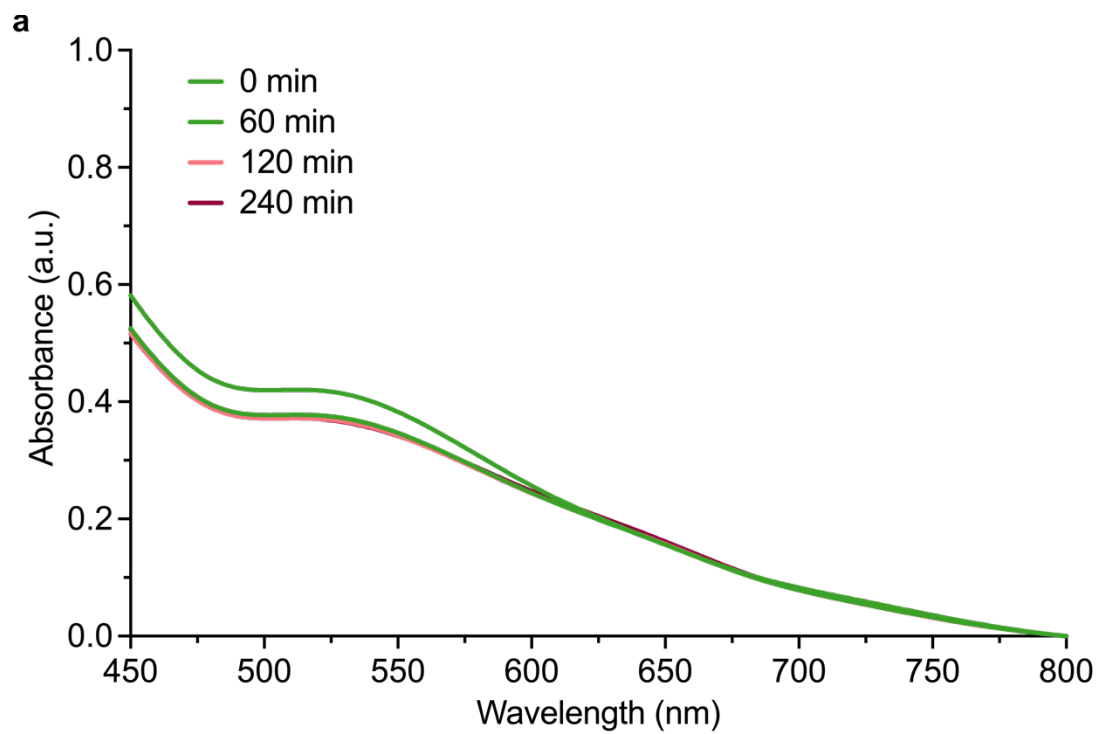
Figure S5. Visible absorption spectra of the solutions of **C₁₂RhMOP+NO** (a) and **C₁₂RhMOP-biz+NO** (b) in toluene, after keeping in the dark during at several times.
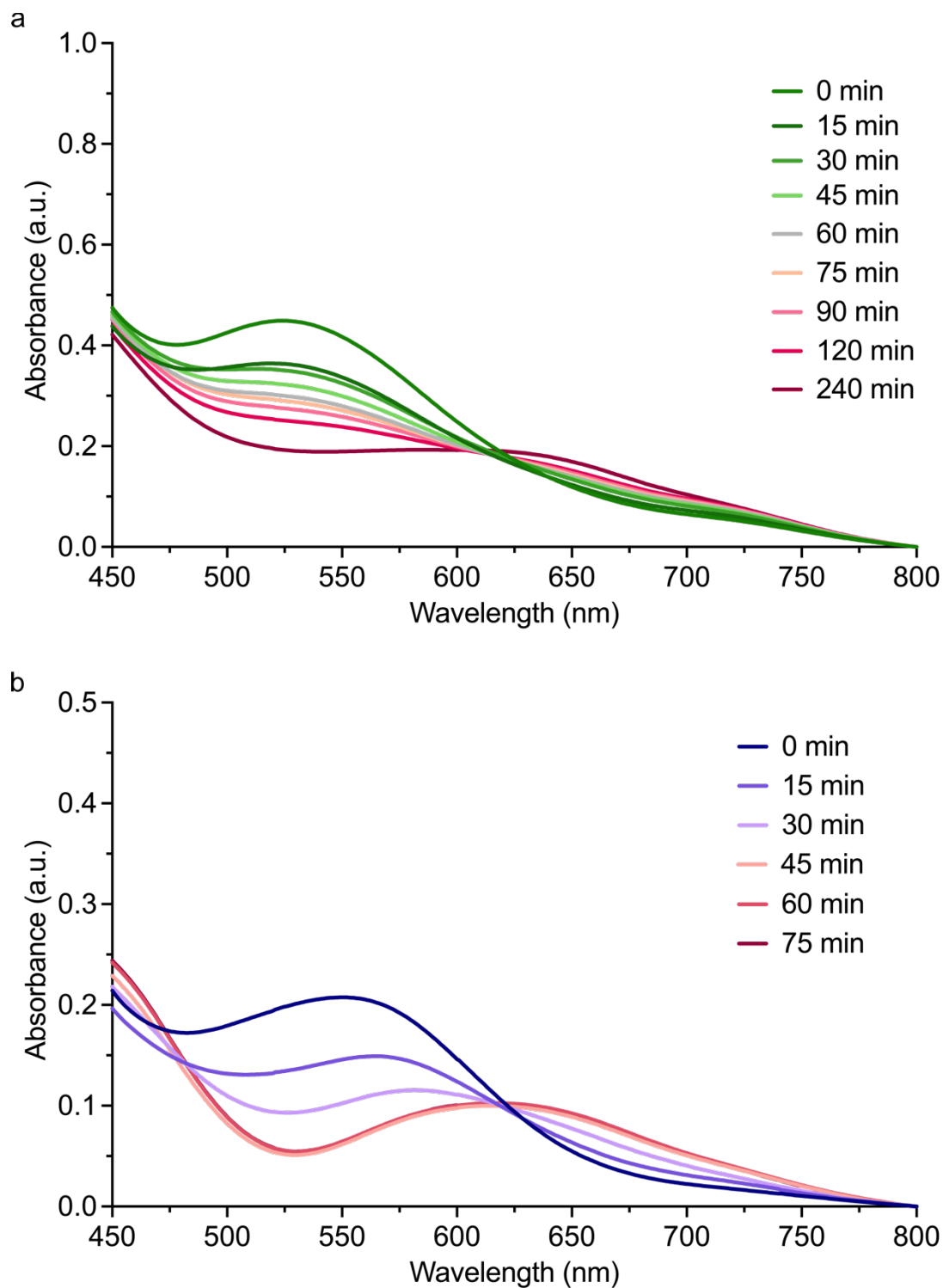
Figure S6. Visible absorption spectra of the solutions of **C₁₂RhMOP+NO** (a) and **C₁₂RhMOP-biz+NO** (b) in toluene, after being irradiated with light ($\lambda = 300$-600 nm) at several times.
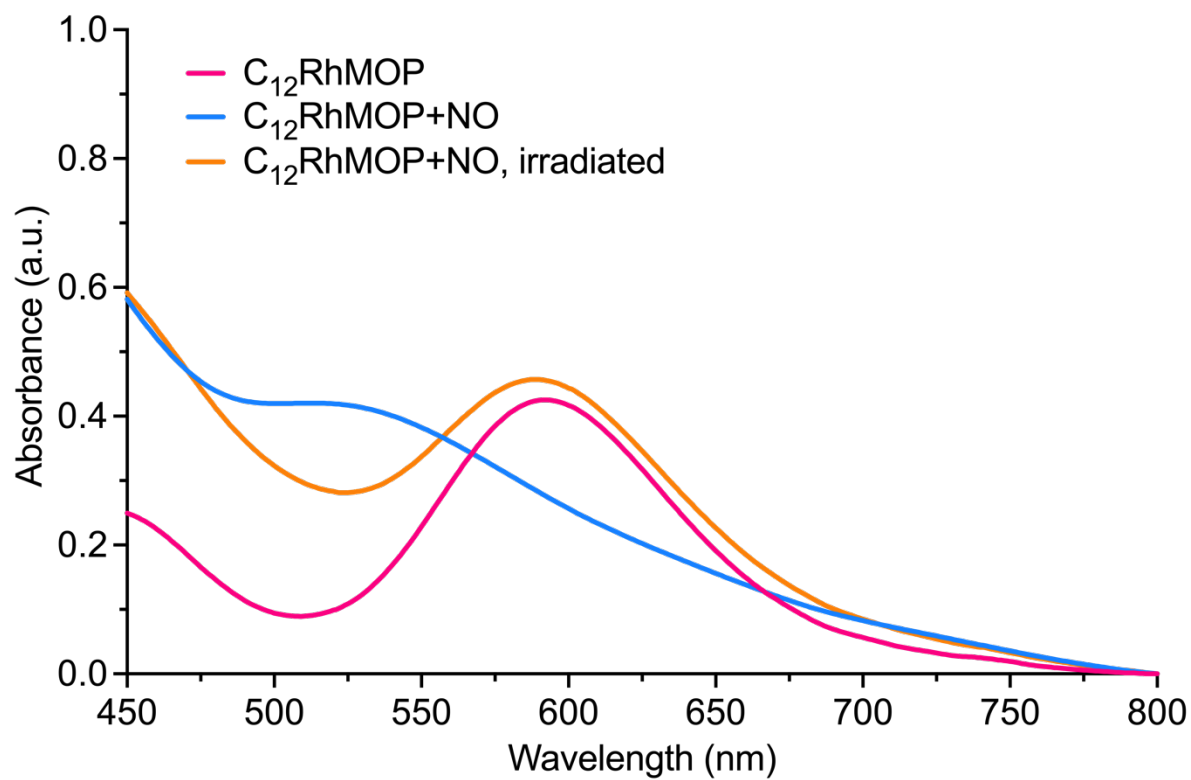
Figure S7. Visible absorption spectra of the solutions of **C$_{12}$RhMOP+NO, irradiated** compared to **C$_{12}$RhMOP** and **C$_{12}$RhMOP+NO**; Samples are dissolved in toluene, and irradiated with light (λ = 300-600 nm)
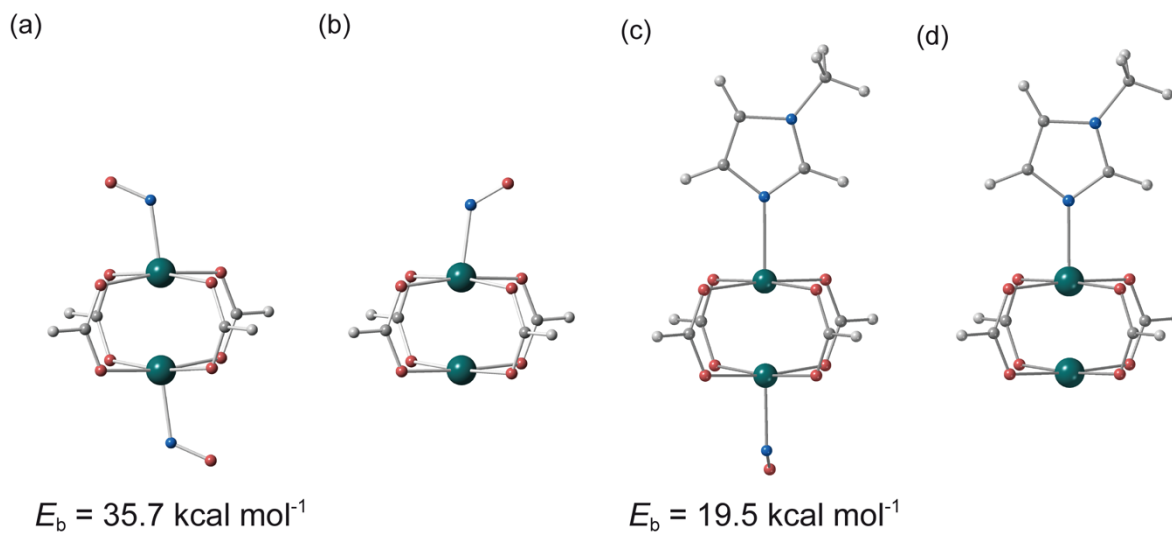
E_b = 35.7 kcal mol^{-1} E_b = 19.5 kcal mol^{-1}

Figure S8. Optimized structures of (a) Rh$_2$(HCO$_2$)$_4$(NO)$_2$, (b) Rh$_2$(HCO$_2$)$_4$(NO), (c) Rh$_2$(HCO$_2$)$_4$(NO)(Me-Im), and (d) Rh$_2$(HCO$_2$)$_4$(Me-Im).

Table S3. Binding energy, bond length (in Ångströms) and bond index determined by DFT calculations.

Ligand	Binding energy (Kcal mol^{-1})	Bond index of NO-Rh	Bond length of NO-Rh (Å)	Bond index of Rh-Rh	Bond length of Rh-Rh (Å)
RhPW	0	-	-	0.904	2.402
NO & MeIm	19.5	0.802	2.012	0.519	2.502
NO & NO	35.7	1.006	1.952	0.272	2.597

a)
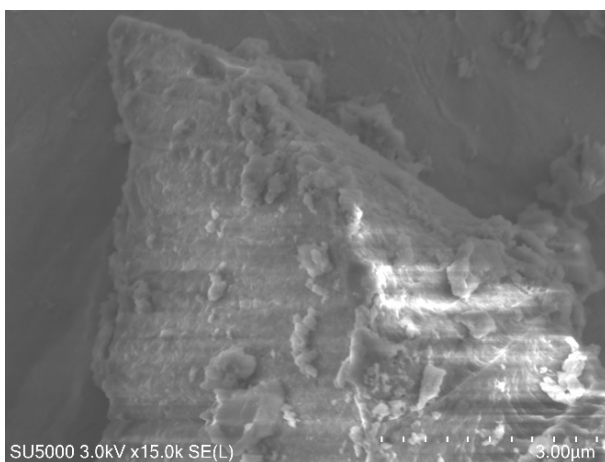
b)
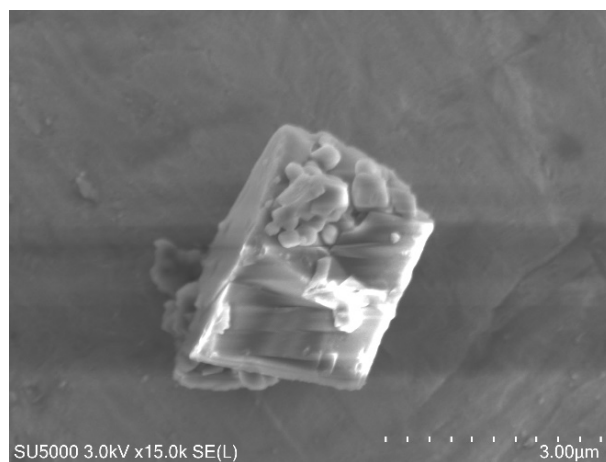
Figure S9. SEM images of a) **C$_{12}$RhMOP** and b) **C$_{12}$RhMOP-biz**. Scale bar = 3 μm.

Table S4. NO-release of the materials prepared in comparison with other porous materials with open metal sites proposed as NO-releasing frameworks.

| Sample	Trigger	NO-release (mmol g^{-1})	Cumulative release (%)	Reference
C$_{12}$RhMOP+NO	Wet gas	0.42	19.9	This work
	Light	0.10	4.8	
C$_{12}$RhMOP-biz+NO	Wet gas	0.16	12.9	
	Light	0.11	8.4	
C$_{12}$RhMOP-CPP+NO	Wet gas	0.11	11.2	
	Light	0.20	19.8	
HKUST-1	Wet gas	0.002	0.1	[8]
Co-CPO	Wet gas	6.0	100.0	[9]
Ni-CPO	Wet gas	7.0	100.0	
MIL-88-A	Wet gas	0.12	4.8	[10]
MIL-88-B	Wet gas	0.0	0.0	
MIL-88-B-NO$_2$	Wet gas	0.14	14.0	
MIL-88-B-2OH	Wet gas	0.12	12.0	
Fe$_2$(dobdc)	Wet gas	4.0	64.5	[11]

a

b
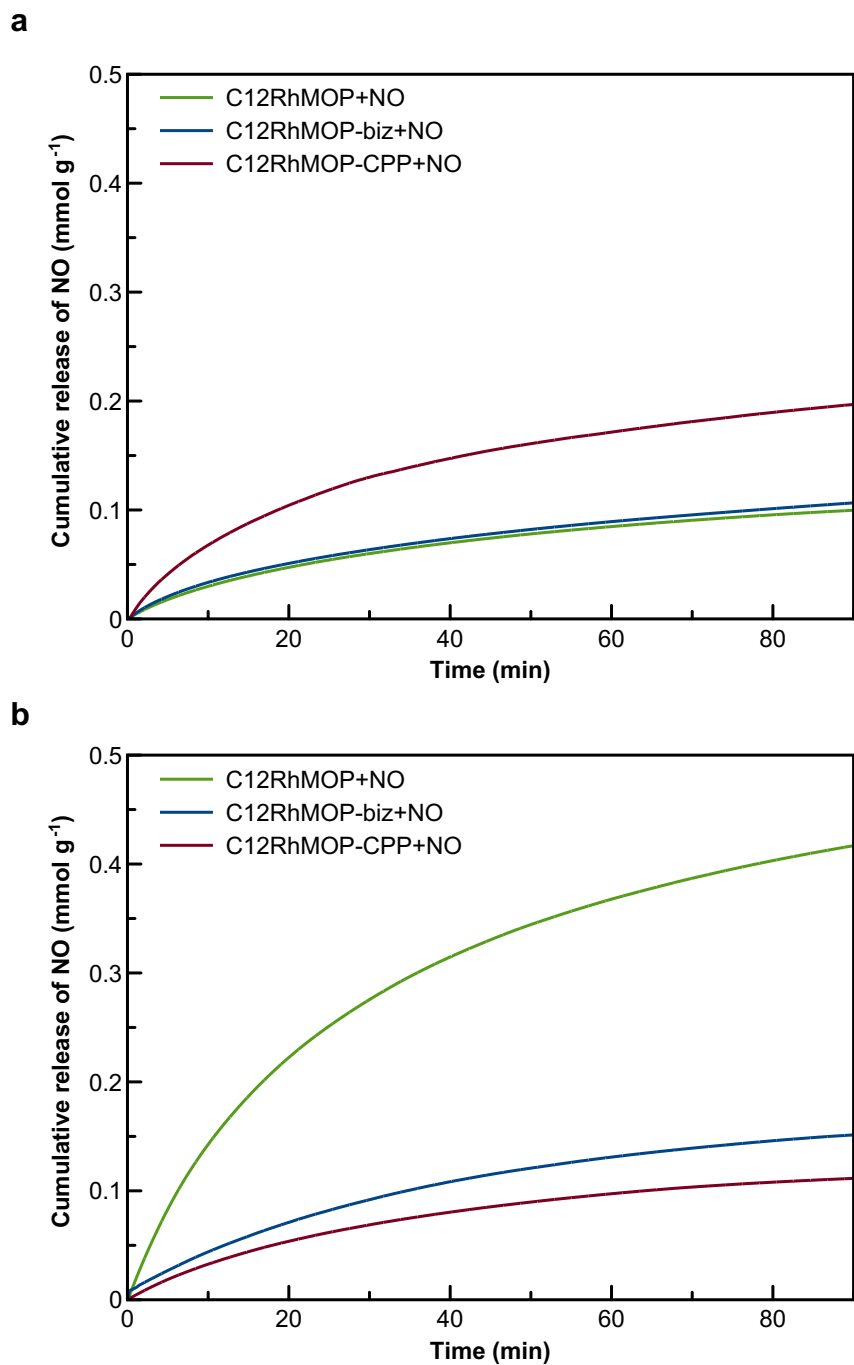
Figure S10. Cumulative NO release expressed as mmol of NO per gram of material from **C₁₂RhMOP+NO** (green curves), **C₁₂RhMOP-biz+NO** (blue curve) and **C₁₂RhMOP-CPP+NO** (purple curve) in solid state: (a) under visible light and (b) in contact with a nitrogen flow saturated with water.
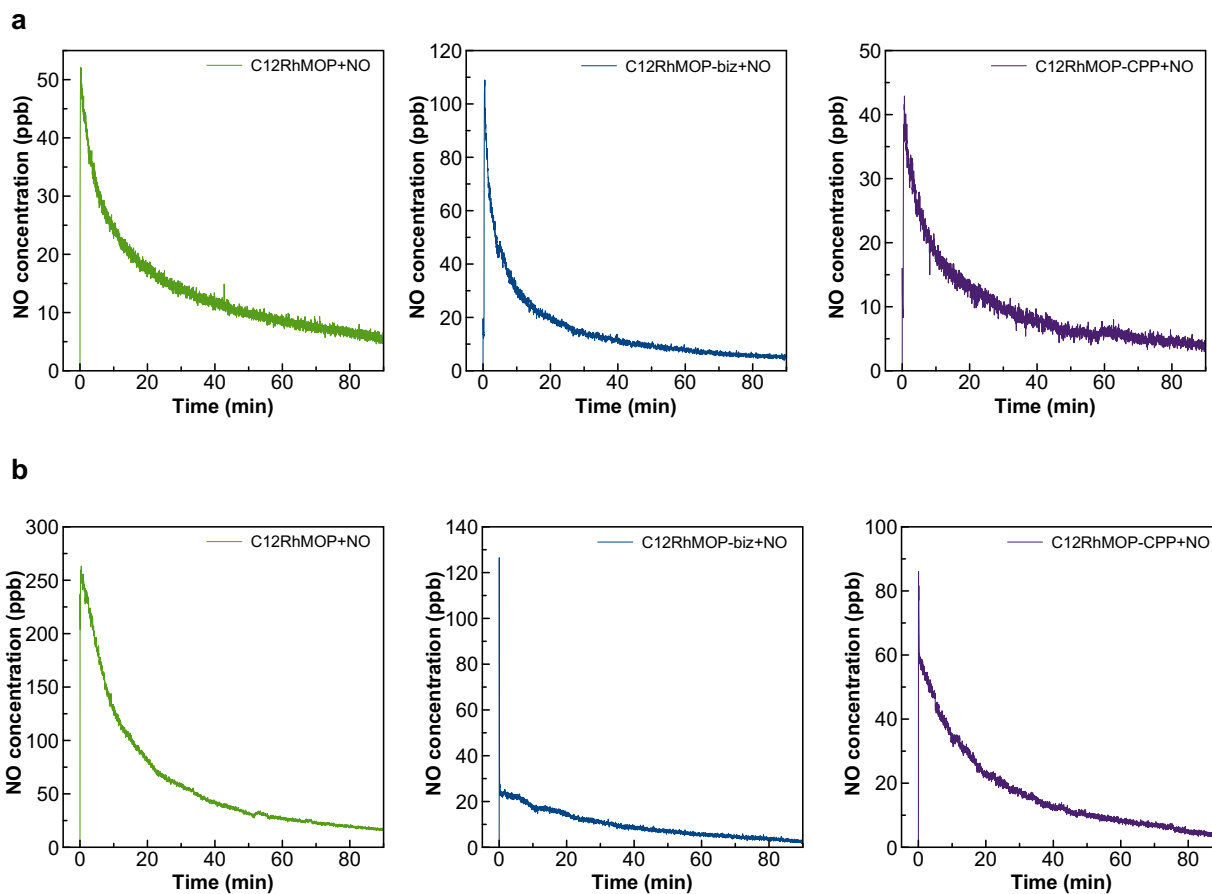
a

b

Figure S11. Nitric oxide concentration in the nitrogen flow expressed as ppb during the NO-release studies under (a) light irradiation and (b) in contact with a nitrogen flow saturated with water. **C₁₂RhMOP+NO** (green curves), **C₁₂RhMOP-biz+NO** (blue curve) and **C₁₂RhMOP-CPP+NO** (purple curve)

References

(1)   Dhal, P. K.; Arnold, F. H. Metal-Coordination Interactions in the Template-Mediated Synthesis of Substrate-Selective Polymers: Recognition of Bis(Imidazole) Substrates by Copper(II) Iminodiacetate Containing Polymers. *Macromolecules* **1992**, *25* (25), 7051–7059.

(2)   Carné-Sánchez, A.; Craig, G. A.; Larpent, P.; Hirose, T.; Higuchi, M.; Kitagawa, S.; Matsuda, K.; Urayama, K.; Furukawa, S. Self-Assembly of Metal-Organic Polyhedra into Supramolecular Polymers with Intrinsic Microporosity. *Nat. Commun.* **2018**, *9* (1), 1–8.

(3)   Furukawa, S.; Horike, N.; Kondo, M.; Hijikata, Y.; Carné-Sánchez, A.; Larpent, P.; ...; Kitagawa, S. Rhodium–Organic Cuboctahedra as Porous Solids with Strong Binding Sites. *Inorg. Chem.* **2016**, 55 (21), 10843-10846.

(4)   Zhao, Y.; Truhlar, D. G. A New Local Density Functional for Main-Group Thermochemistry, Transition Metal Bonding, Thermochemical Kinetics, and Noncovalent Interactions. *J. Chem. Phys.* **2006**, 125 (19).

(5)   Dolg, M.; Wedig, U.; Stoll, H.; Preuss, H. Energy-Adjusted Ab Initio Pseudopotentials for the First Row Transition Elements. *J. Chem. Phys.* **1987**, 86 (2), 866-872.

(6)   Frisch, M. J.; Trucks, G. W.; Schlegel, H. B.; Scuseria, G. E.; Robb, M. A.; Cheeseman, J. R.; ...; Fox, D. J. Gaussian 16 Revision A.03, **2016**, Gaussian Inc., Wallingford CT.

(7)   Boys, S. F.; Bernardi, F. J. M. P. The Calculation of Small Molecular Interactions by the Differences of Separate Total Energies. Some Procedures with Reduced Errors. *Mol. Phys.* **1970**, 19 (4), 553-566.

(8)   Xiao, B.; Wheatley, P. S.; Zhao, X.; Fletcher, A. J.; Fox, S.; Rossi, A. G.; Megson, I. L.; Bordiga, S.; Regli, L.; Thomas, K. M.; Morris, R. E. High-Capacity Hydrogen and Nitric Oxide Adsorption and Storage in a Metal-Organic Framework. *J. Am. Chem. Soc.* **2007**, *129* (5), 1203–1209.

(9)   McKinlay, A. C.; Xiao, B.; Wragg, D. S.; Wheatley, P. S.; Megson, I. L.; Morris, R. E. Exceptional Behavior over the Whole Adsorption-Storage-Delivery Cycle for NO in Porous Metal Organic Frameworks. *J. Am. Chem. Soc.* **2008**, *130* (31), 10440–10444.

(10)   McKinlay, A. C.; Eubank, J. F.; Wuttke, S.; Xiao, B.; Wheatley, P. S.; Bazin, P.; Lavalley, J. C.; Daturi, M.; Vimont, A.; De Weireld, G.; Horcajada, P.; Serre, C.; Morris, R. E. Nitric Oxide Adsorption and Delivery in Flexible MIL-88(Fe) Metal-Organic Frameworks. *Chem. Mater.* **2013**, *25* (9), 1592–1599.

(11)   Bloch, E. D.; Queen, W. L.; Chavan, S.; Wheatley, P. S.; Zadrozny, J. M.; Morris, R.; Brown, C. M.; Lamberti, C.; Bordiga, S.; Long, J. R. Gradual Release of Strongly Bound Nitric Oxide from Fe2(NO)2(Dobdc). *J. Am. Chem. Soc.* **2015**, *137* (10), 3466–3469.